

COMPUTER ANALYSIS OF CURRENT SOURCE INVERTER INDUCTION MOTOR DRIVE SYSTEMS*

By

M. M. EL-SAYED

Department of Electric Machines, Technical University, Budapest

(Received June 22, 1976)

Presented by Prof. Dr. Gyula RETTER

Introduction

The known concept of supplying an induction motor from a static current source converter results in ac drive performance with several important advantages over the more familiar voltage fed inverter. An ac drive using such a current source inverter is shown in Fig. 1. Basically, it consists of a controlled bridge rectifier, a simple dc filter choke, and an inverter bridge. The controlled rectifier and filter choke combine to form a dc regulator which supplies a regulated dc current to the inverter terminals. The inverter directs this regulated current into the appropriate motor phases at some desired frequency. The inverter's switches are controlled by logic circuits piloted by the machine's rotating speed.

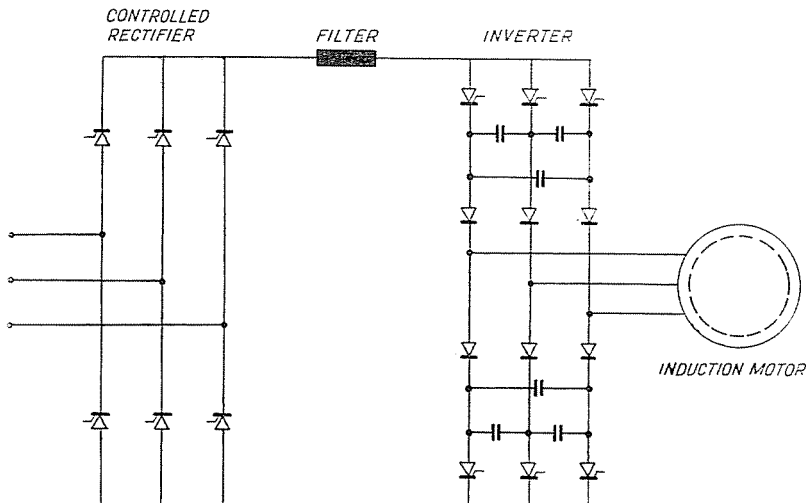


Fig. 1. Schematic diagram of converter power circuit

* Fellowship research done at the Department of Electric Machines under the guidance of Ass. Prof. Dr. József Lázár.

Numerous investigations have enabled the determination of the steady state characteristics of this new autopiloted-converter-machine group. Analysis of motor performance has been conducted by considering only the fundamental components of the ac line current [3, 4]. The terminal characteristics of an induction motor when fed with "quasi-square" current wave form have been explained using an analytical approach with a series equivalent circuit of induction motor to the n -th harmonic [6]. An alternative procedure for the steady state analysis results in a closed form solution assuming ideal current filtering and constant rotor speed [8].

In this paper a space-vector representation of motor and inverter is introduced [1]. The introduction of space-vector representation gives a better understanding of both stationary and transient phenomena that take place in an induction motor. Here this is very useful for understanding the interaction between inverter and motor, especially regarding the conduction states of the inverter diodes. The three phase quantities can be shown in one picture and the time functions can be easily obtained by a simple projecting procedure. With state variable approach the differential equations for the system are written using all usual energy storages and exact results can be obtained. A digital computations are needed to solve the non-linear differential equations.

Basic equations of induction machine

For static frequency converters with current source inverters, the inverter commutations take place on the ac side involving the motor windings. Therefore no analysis of the inverter can be made without considering the operation conditions of the motor. In that respect the current source inverters differ from voltage source inverters, that generally can be analyzed separately, that is, without much consideration of load characteristics. In the following analysis a space vector equivalent circuit represents the induction machine shown in Fig. 2. For that case the saturation and eddy current effects are neglected and the rotor parameters can be reduced to the stator side in such a way that the leakage inductance of the rotor has been reduced to zero. Since the inverter is connected to the stator winding it is convenient to apply a stationary reference frame fixed to the stator. In this co-ordinate system the fundamental equations of induction machine based on the space-vector approach are given by

$$\bar{u}_s = \bar{i}_s R_s + \frac{d\bar{\psi}_s}{dt} \quad (1)$$

$$0 = \bar{i}_r R_r + \frac{d\bar{\psi}_r}{dt} - j\omega \bar{\psi}_r \quad (2)$$

where:

- $\bar{\psi}_s, \bar{i}_s, \bar{u}_s$ are the stator flux, current, and voltage;
- $\bar{\psi}_r, \bar{i}_r, \omega$ are the rotor flux, current, and rotor angular velocity;
- R_s, R_r are the stator and rotor resistances, respectively.

The stator and rotor currents expressed in terms of stator and rotor flux are:

$$\bar{i}_s = \frac{\bar{\psi}_s - \bar{\psi}_r}{L'_s} \tag{3}$$

$$\bar{i}_r = \frac{\bar{\psi}_r - (1 - \sigma)\bar{\psi}_s}{L'_r} \tag{4}$$

where:

$\sigma = L'_s/L_s$ the leakage factor; L'_s and L'_r are the stator and rotor transient inductances, respectively. For the exact solution the speed variation must be taken into consideration, especially in the case of low frequencies; requiring the equation of motion:

$$T - T_l = T_{sn} \frac{d\omega}{dt} \tag{5}$$

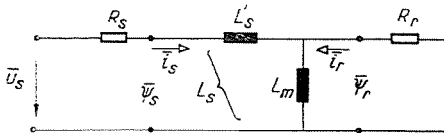


Fig. 2. Equivalent circuit of induction machine

where T_l is the load torque assumed to be constant, and T_{sn} is the nominal starting time of the motor. T is the electromechanical torque and in per unit system, it is equal to

$$T = \frac{1}{L'_s} (\bar{\psi}_r \times \bar{\psi}_s) \tag{6}$$

where \times means vector product.

Analysis of current-fed inverter circuit

The current source type of frequency converter has been described in detail in [5, 6] and will not be repeated here except for emphasizing that only two thyristors are on at once, each one conducting the dc link current i_d for 120° . A thyristor is commutated by firing the adjacent thyristor in the next phase. Fig. 3 is a simplified scheme of six-step current-mode inverter power circuit, where for the sake of simplicity the delta connection of the capacitors is replaced by the equivalent star one. The arrows indicate

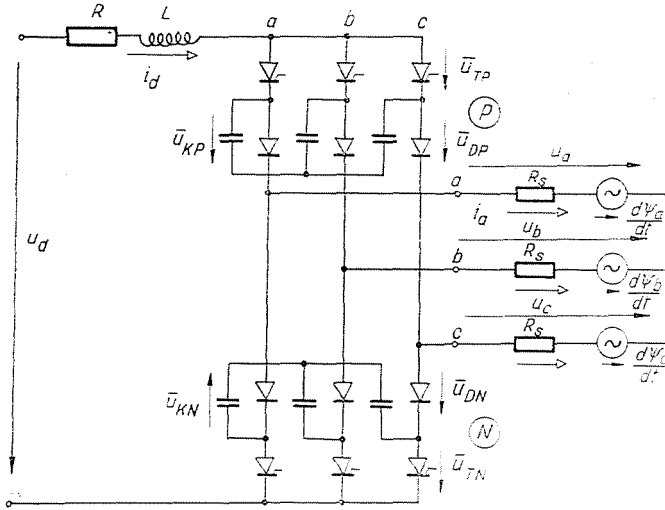


Fig. 3. Simplified schematic of current mode inverter power circuit

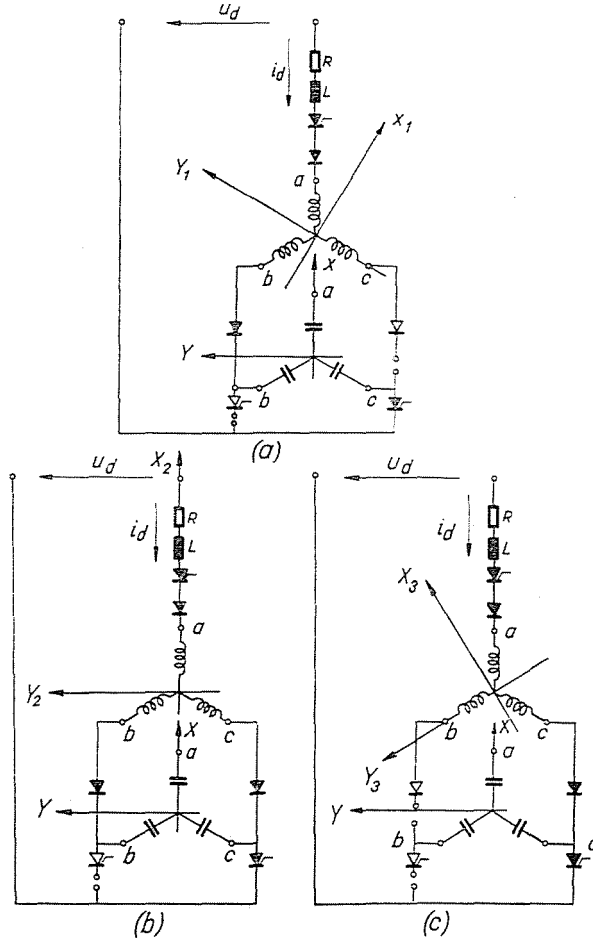


Fig. 4. Modes of operation

the chosen positive direction of voltage and current of each element in the circuit. Thyristor, diode, and capacitor are abbreviated by symbols T , D and K , respectively. Fig. 4 illustrates the three different conduction states which occur during one-sixth of the total period. However, because of periodicity, it is quite sufficient to study one-sixth period where the data of others may be obtained through phase and sign changes. A co-ordinate system fixed to the stator is chosen. Utilizing the symmetry of the circuits, the co-ordinate system is fixed to the symmetry axes. Different reference frames are used for different modes of operation as shown in Fig. 4. In each case the state equation represents the system in the form:

$$\frac{dx}{dt} = \mathbf{A} x + b \tag{7}$$

If the machine fluxes are chosen as state variables, then in Eq. (7) \mathbf{A} is the function matrix of the state vector x where:

$$[x]^T = [\psi_{sx} \ \psi_{sy} \ \psi_{rx} \ \psi_{ry} \ u_{KNy} \ \omega] \tag{8}$$

Matrix \mathbf{A} and b differ from one conduction state to another; for the first mode of operation they are given by:

$$\mathbf{A} = \begin{bmatrix} \sigma_1 \frac{1-\sigma}{T_r'} - \frac{1}{T_1} & 0 & -\frac{\sigma_1}{T_r'} + \frac{1}{T_1} & -\sigma_1 \omega & -1 + \sigma_1 & 0 \\ 0 & -\frac{1}{T_r} & \omega & 0 & 0 & 0 \\ \frac{1-\sigma}{T_r'} & 0 & -\frac{1}{T_r'} & -\omega & 0 & 0 \\ 0 & -\frac{1}{T_r} & \omega & 0 & 0 & 0 \\ \frac{1}{\Omega^2} & 0 & -\frac{1}{\Omega^2} & 0 & 0 & 0 \\ -\frac{\psi_{ry}}{L_s' T_{sn}} & \frac{\psi_{rx}}{L_s' T_{sn}} & 0 & 0 & 0 & 0 \end{bmatrix} \tag{9}$$

$$[b]^T = \left[\frac{1-\sigma_1}{\sqrt{3}} u_d \quad 0 \quad 0 \quad 0 \quad 0 \quad \frac{T_l}{T_{sn}} \right] \tag{10}$$

In case of second mode of operation, matrices \mathbf{A} and b are as follows:

$$A = \begin{bmatrix} \sigma_2 \frac{1-\sigma}{T_r'} - \frac{1}{T_2} & 0 & -\frac{\sigma_2}{T_r'} + \frac{1}{T_2} & -\sigma_2 \omega & -\frac{1+\sigma_2}{3} & 0 \\ 0 & -\frac{1}{T_s'} & 0 & \frac{1}{T_s'} & 1 & 0 \\ \frac{1-\sigma}{T_r'} & 0 & -\frac{1}{T_r'} & -\omega & 0 & 0 \\ 0 & \frac{1-\sigma}{T_r'} & \omega & -\frac{1}{T_r'} & 0 & 0 \\ \frac{1}{\sqrt{3}\Omega^2} & -\frac{1}{\Omega^2} & -\frac{1}{\sqrt{3}\Omega^2} & \frac{1}{\Omega^2} & 0 & 0 \\ -\frac{\psi_{ry}}{L_s' T_{sn}} & \frac{\psi_{ry}}{L_s' T_{sn}} & 0 & 0 & 0 & 0 \end{bmatrix} \quad (11)$$

$$[b]^T = \begin{bmatrix} \frac{2(1-\sigma_2)}{3} u_d & 0 & 0 & 0 & 0 & -\frac{T_l}{T_{sn}} \end{bmatrix} \quad (12)$$

To the third mode the following relations hold true:

$$A = \begin{bmatrix} \sigma_1 \frac{1-\sigma}{T_r'} - \frac{1}{T_1} & 0 & -\frac{\sigma_1}{T_r'} + \frac{1}{T_1} & -\sigma_1 \omega & 0 & 0 \\ 0 & -\frac{1}{T_r} & \omega & 0 & 0 & 0 \\ \frac{1-\sigma}{T_r'} & 0 & -\frac{1}{T_r'} & -\omega & 0 & 0 \\ 0 & -\frac{1}{T_r} & \omega & 0 & 0 & 0 \\ 0 & 0 & 0 & 0 & 0 & 0 \\ -\frac{\psi_{ry}}{L_s' T_{sn}} & \frac{\psi_{rx}}{L_s' T_{sn}} & 0 & 0 & 0 & 0 \end{bmatrix} \quad (13)$$

$$[b]^T = \begin{bmatrix} \frac{1-\sigma_1}{\sqrt{3}} u_d & 0 & 0 & 0 & 0 & -\frac{T_l}{T_{sn}} \end{bmatrix} \quad (14)$$

where:

T_s' and T_r' are the stator and rotor transient time constants, respectively;
 T_r the rotor open-circuit time constant;

$$\sigma_1 = \frac{L}{L + 2L_s'}, \quad T_1 = \frac{L + 2L_s'}{R + 2R_s};$$

$$\sigma_2 = \frac{L}{L + \frac{3}{2}L'_s}, \quad T_2 = \frac{L + \frac{3}{2}L'_s}{R + \frac{3}{2}R'_s}, \quad \Omega = \frac{1}{\sqrt{L'_s C}};$$

u_d is a constant value (average) of the dc voltage; and L and R are the choke parameters.

The first mode of operation prevails (see Fig. 4/a) as long as condition $u_{Kbc} - u_{bc} \leq 0$ is fulfilled. The end of this interval is determined when diode c in the negative side is coming into conduct and consequently the b - c terminal voltage of the capacitors is connected across the b - c terminals of the induction machine as shown in Fig. 4/b. At this point the current begins to transfer from phase b to phase c during the diode commutation period until the current in diode of phase b has been driven to zero; i.e. $i_b = 0$. Fig. 4/c describes the last mode of operation where phase c assumes the full value of the dc current i_d . The interval of this conduction state is determined so that the length of the stroke τ equals one-sixth of the total period.

Steady state characteristics

The state equations describing the system are non-linear; therefore an iteration method using the periodicity condition is applied to obtain a steady state operating point. This iteration method is principally based on modifying the initial state vector \mathbf{x}_{st} by a small variation $\Delta\mathbf{x}_{st}$ to obtain the same at the end of the interval in a synchronous reference frame. The procedure was the following:

$$\begin{aligned} \mathbf{x}_{st} &\rightarrow \text{Runge-Kutta} \rightarrow \mathbf{x}_{end} \\ dev &= \mathbf{x}_{end} - \mathbf{x}_{st} \\ \Delta\mathbf{x}_{end} &= \mathbf{Z} \Delta\mathbf{x}_{st} \\ \mathbf{x}_{st} + \Delta\mathbf{x}_{st} &= \mathbf{x}_{end} + \Delta\mathbf{x}_{end} \\ \Delta\mathbf{x}_{st} &= [\mathbf{I} - \mathbf{Z}]^{-1} dev \\ \mathbf{x}_{st(new)} &= \mathbf{x}_{st} + \Delta\mathbf{x}_{st} \end{aligned} \tag{15}$$

This needs the knowledge of the state transition matrix \mathbf{Z} of the system. If the system is piece-wise linear, the state matrix can be calculated in explicit form. If the system is nonlinear, then the matrix \mathbf{Z} can be computed by numerical solution of the state equation [7]. Already few of such iteration yield an exact result. Since the open loop is unstable especially at higher frequencies, this method is superior in achieving the steady state operating

condition. The problem is solved using a digital computer and the state equations have been computed by means of fourth-order Runge—Kutta routine. For the solution, u_d and T_l are given at each frequency and the initial value of state variables has been determined using an approximate method [9], based on the neglect of the stator resistance and assuming the dc current to be constant. The calculations were applied on a system with the following parameters in per unit system:

stator resistance	$R_s = 0.05$
rotor resistance	$R_r = 0.045$
magnetizing inductance	$L_m = 2.12$
stator transient inductance	$L' = 0.16$
DC link resistance	$R = 0.05$
DC link inductance	$L = 0.8$
commutation capacitor	$C = 0.09$
nominal starting time	$T_{sn} = 60$

Two operating points representing motor and generator steady state operations were obtained at two different frequencies: 50 cps and 5 cps, respectively. At the higher frequency the calculation was performed using the approximate method too. At the lower frequency this method is not valid because the stator, and rotor resistances and the dc choke parameters must be taken into consideration. In each case the rotor flux is held constant at a unit value. Figs 5/a to 5/c show the Park-vector loci at 50 cps for each of \vec{i}_s , \vec{u}_s , \vec{u}_K ,

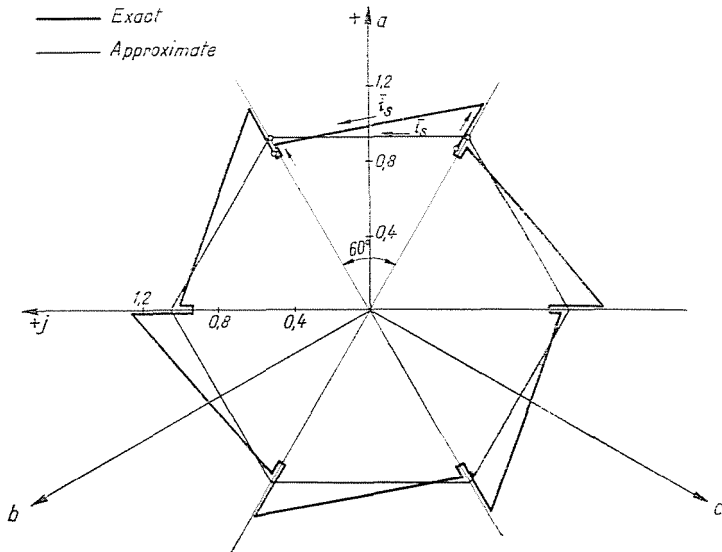


Fig. 5/a Vector locus of stator current for motor operation: $T_l = 0.85$, $f = 50$ cps

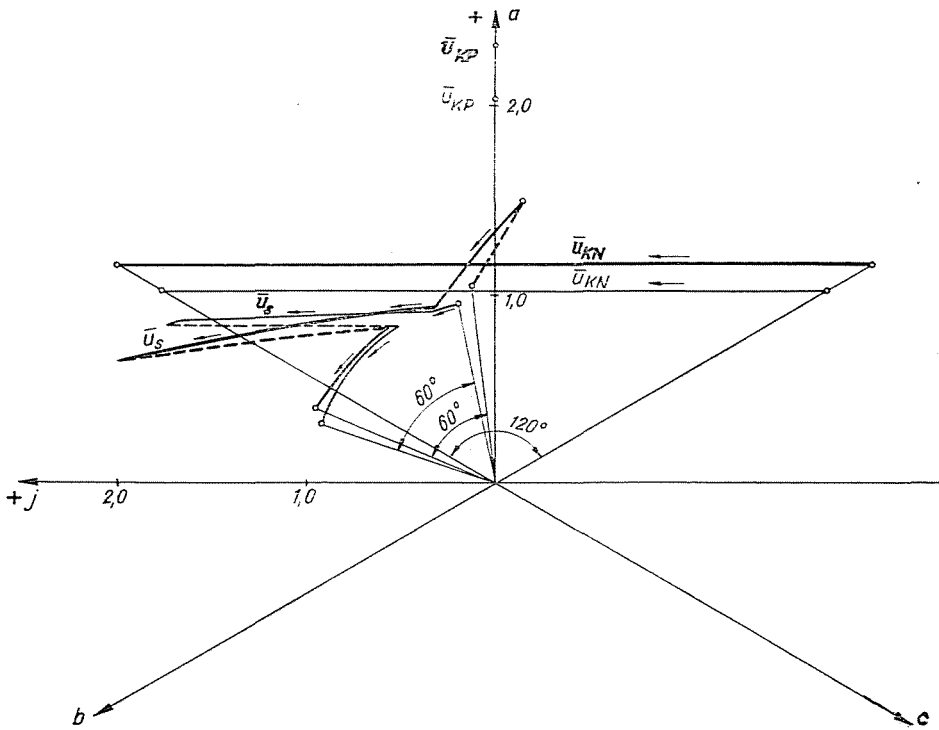


Fig. 5/b Vector loci of stator and capacitor voltages

and \bar{u}_D in case of motor operation at load torque $T_l = 0.85$; (in this per unit system the rated torque 0.73). The projection of vectors on the phase-axes gives the momentary phase quantities. Figs 5/d to 5/f show the time function of dc current, voltage of phase a , and torque, respectively. Fig. 6 represents the generator condition at the same frequency and load torque. Figs 6/a and 6/b show the Park-vector loci of \bar{i}_s , \bar{u}_s , \bar{u}_h and \bar{u}_D ; Fig. 6/c shows the time function of the torque. In all the figures the exact result is shown by a thick line while the thin line represents the approximate one. Figure 7/a shows the Park-vector loci of stator current and stator voltage for motor and generator operation at $T_l = 0.85$ and $f = 5$ cps. The torque and speed periodical time functions are shown in Fig. 7/b for the same operating points. For the reason of periodicity the vector loci are given for one-sixth of the total period. Figure 5/a shows the Park-vector locus of one period.

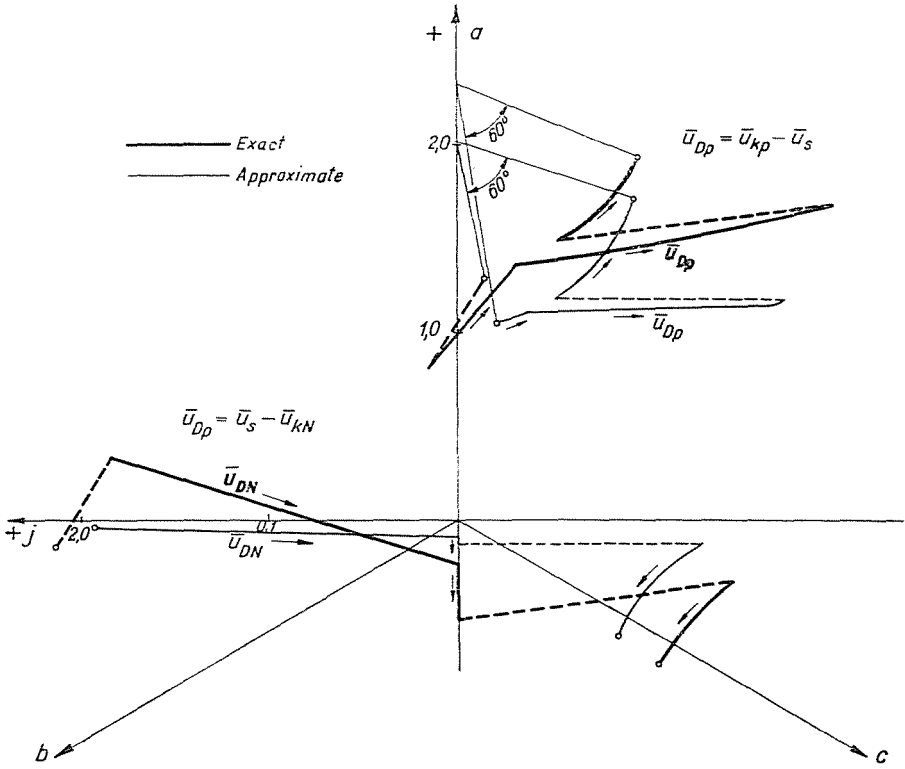


Fig. 5/c Vector locus of diode voltage

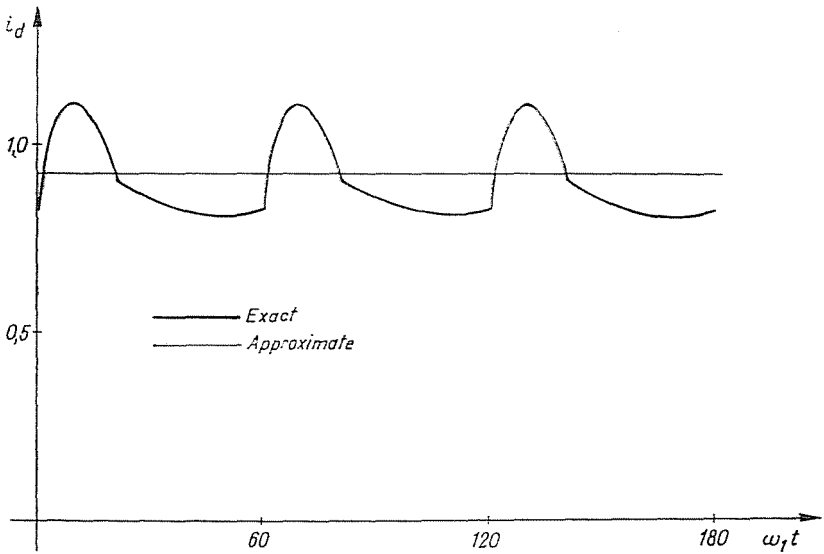


Fig. 5/d DC link current

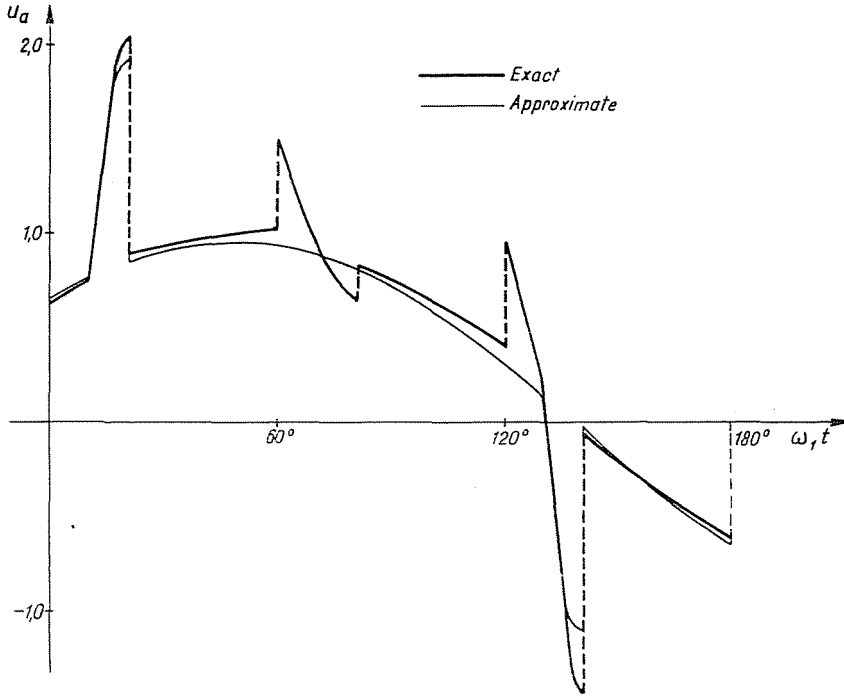


Fig. 5/e Stator voltage of phase a

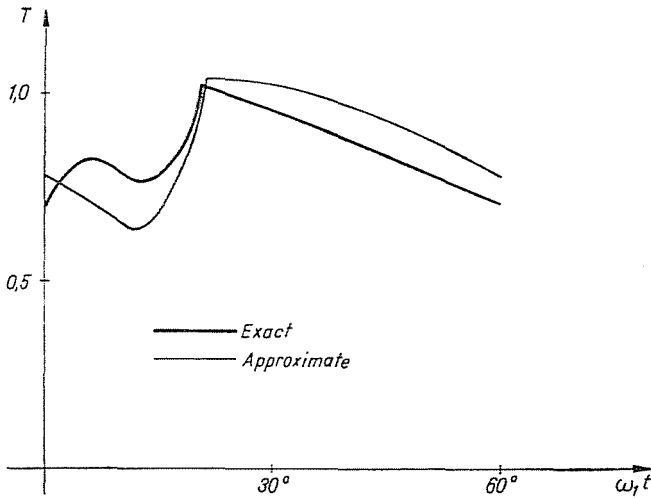


Fig. 5/f Torque time function

Comparison between exact and approximate results

For designing the inverter circuit the rated voltages of the thyristors and diodes are required. They are greatly dependent on how much the maximum value of the capacitor voltages can be reached. From the inverter circuit it follows that the voltage of any diode is equal to the difference of a stator terminal voltage and capacitor line voltage. The instantaneous values of the diode voltages are simply obtained by projecting \bar{u}_{DN} and \bar{u}_{DP} vectors on the resultant (line) direction of the phase axis; the greatest of these projections gives the maximum diode voltage. Figure 6/b shows that higher diode voltages occur in generator mode and the highest of these occurs when the voltage of diode of phase *b* at the positive side of the inverter reaches its maximum value at the end of the second mode of operation. In this case the following relationship holds true.

$$U_{DPb} = - U_{DPa,b} = - \sqrt{3} \text{ (Projection of } \bar{u}_{DP} \text{ in the direction } a, b). \quad (16)$$

The thyristor voltages can be also determined where the voltage of any thyristor is equal to the line voltage of one capacitor. So on side *N* of the

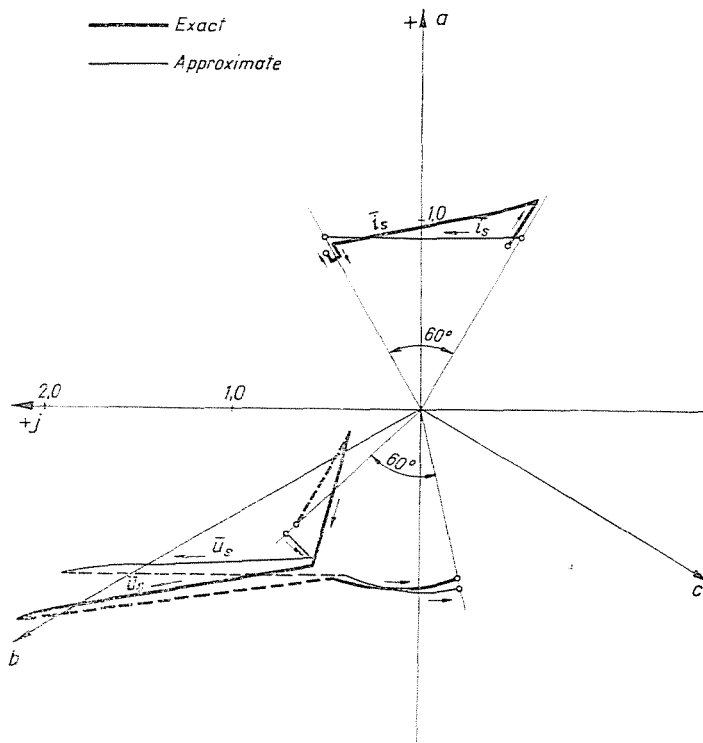


Fig. 6/a Vector loci of stator current and voltage for generator operation: $T_l = -0.85$, $f = 50$ cps

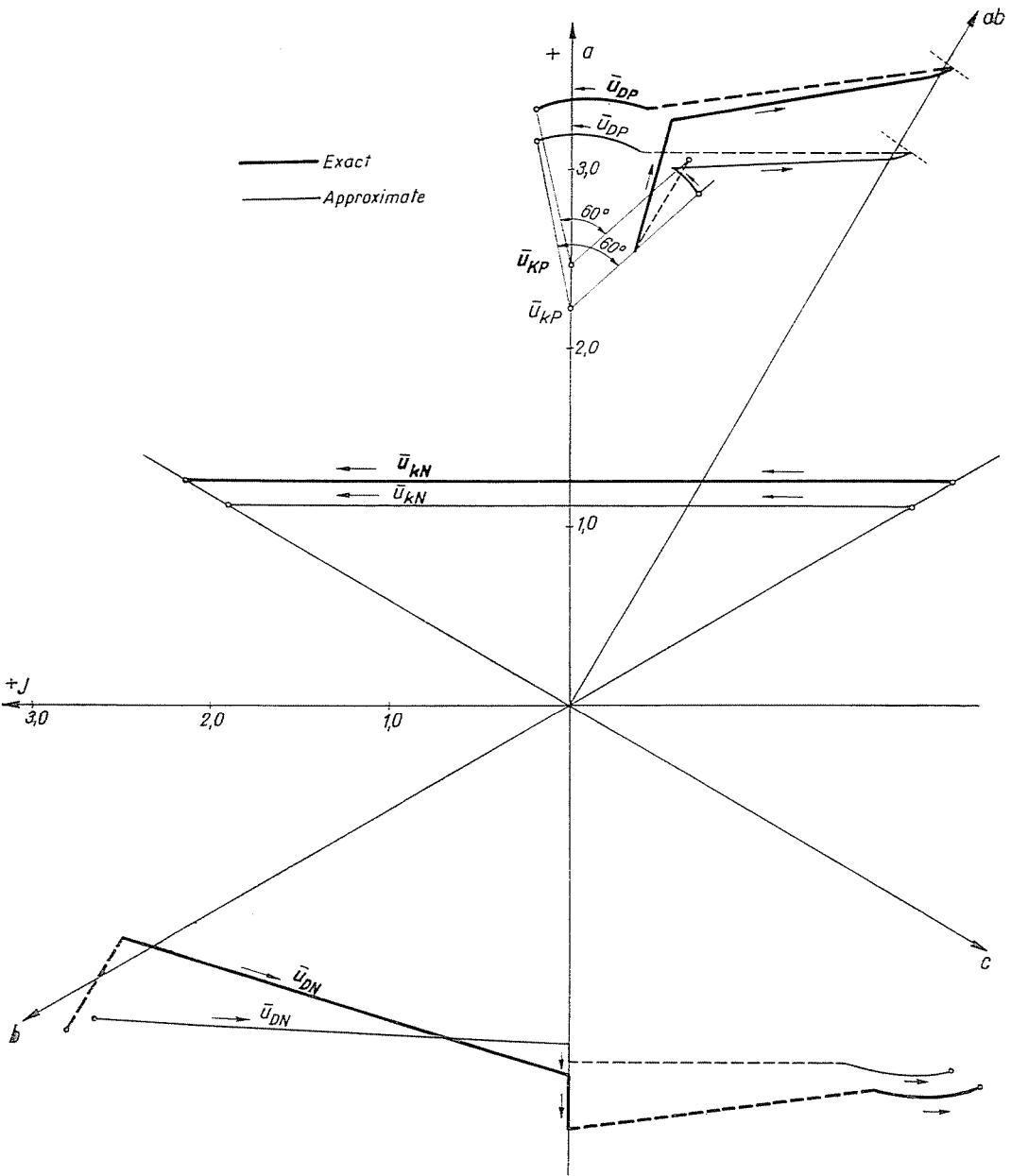


Fig. 6/b Vector loci of diode and capacitor voltages

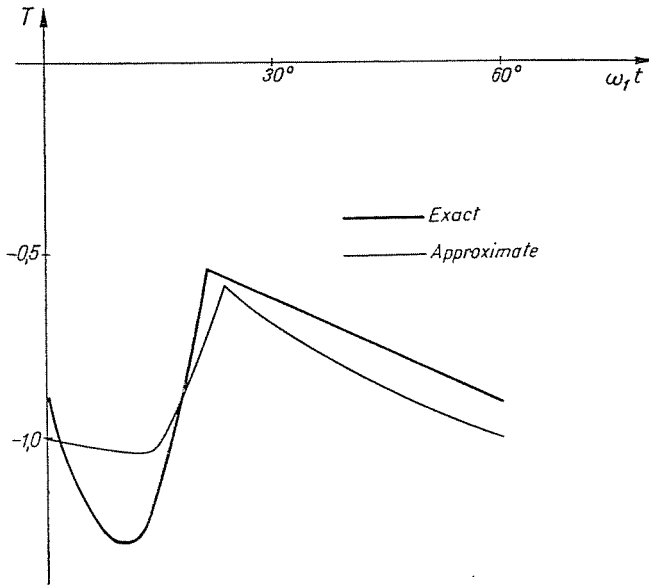


Fig. 6/c Torque time function

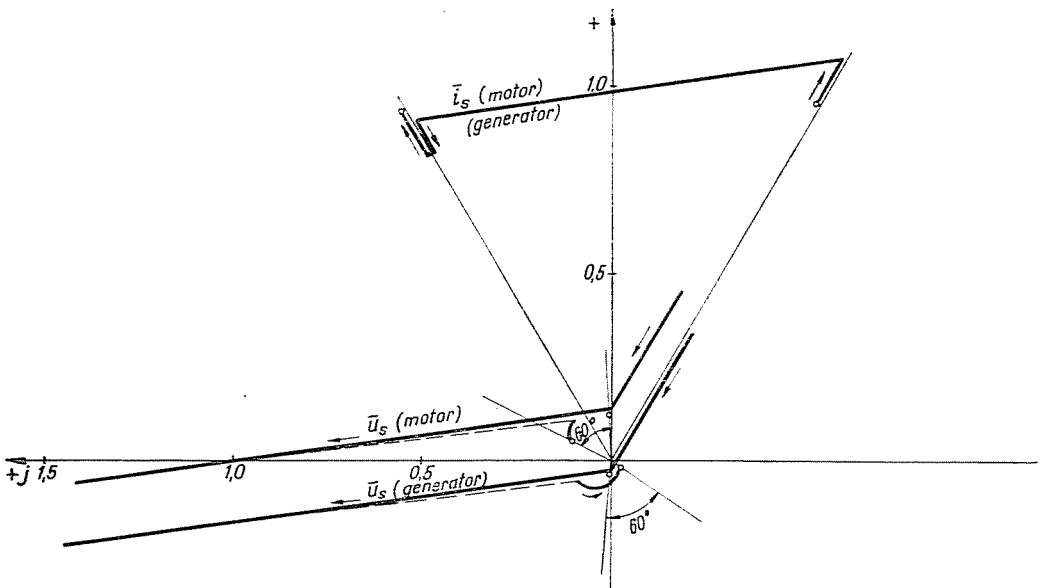


Fig. 7/a Vector loci of stator voltage and current at 5 cps.
 Motor: $T_l = 0.85$; Generator: $T_l = -0.85$

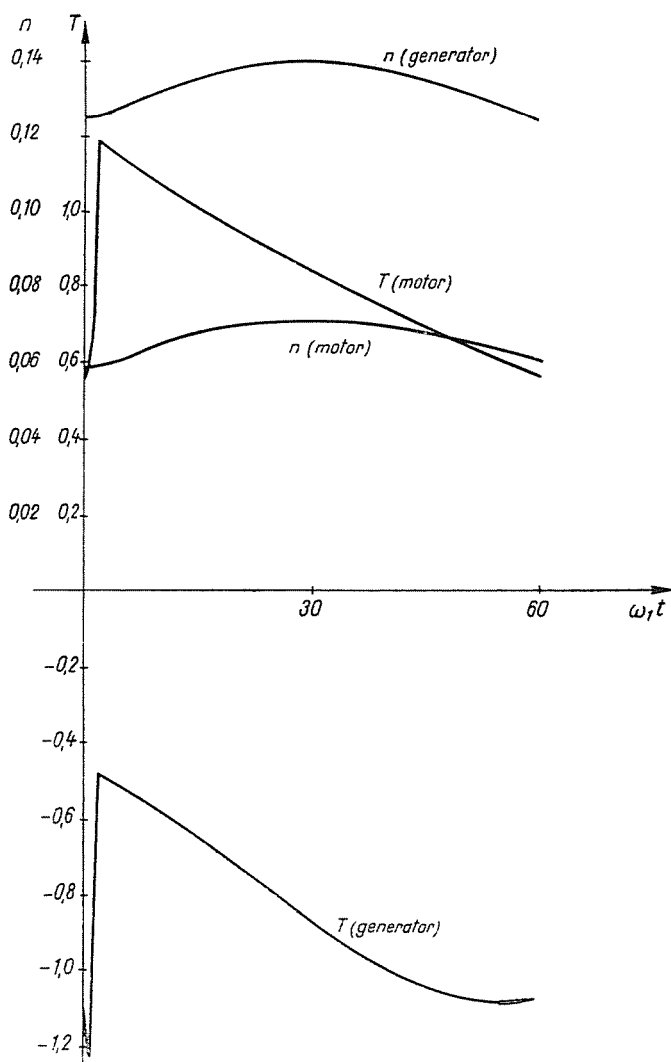


Fig. 7/b Torque and speed time functions

inverter bridge, the voltage of the b thyristor is given by the b - c projection of the \bar{u}_{KN} capacitor voltage. An important relation for the terminal thyristor voltage both in conducting and non-conducting states can be derived as follows:

$$U_{T(\max)} = \frac{3}{2} |\bar{u}_k|_{\max} \quad (17)$$

Table 1

	Approx.	Exact	Error
U_{Dmax}	6.30	7.25	15%
U_{Tmax}	3.30	3.72	12.7%

Table 1 gives a comparison between diode and thyristor maximal voltages calculated by the exact method and the approximate one. Referring to Fig. 6/b the values are given in per unit system.

Stability investigation

For the solution of the steady state operating condition, the state transition matrix \mathbf{Z} is also determined as mentioned before. The greatest advantage of this method is that state matrix \mathbf{Z} characterizes the dynamic behaviour of the system, too. The eigenvalues of the \mathbf{Z} matrix determine the dynamic performance of the open-loop system. λ_i -s give the variation of components Δx which have the same direction of the eigenvectors of matrix \mathbf{Z} within one stroke. If the absolute value of each eigenvalue is smaller than one, the system is stable; $Z^k \rightarrow 0$. If only one $|\lambda_i| > 1$ the system is unstable and cannot be used without stabilizing feedback. The individual components of vector Δx will vary by λ_i^k , thus an equivalent time constant T_i and oscillation frequency ω_i can be defined by the following expressions [2]:

$$\lambda_i = e\left(-\frac{1}{T_i} + j\omega_i\right), \quad T_i = -\tau \frac{1}{\ln |\lambda_i|}; \quad \omega_i = \frac{\text{arc } \lambda_i}{\tau}. \quad (18)$$

Negative T_i means that the corresponding $|\lambda_i|$ is greater than one, and the higher the value of T_i the closer the value of $|\lambda_i|$ to one. A linear transformation was used to get the state matrix \mathbf{Z} with 9×9 elements corresponding to the nine state variables ψ_{sx} , ψ_{sy} , ψ_{rx} , ψ_{ry} , ω , u_{KNx} , u_{Kpx} , u_{KNy} , and u_{Kpy} representing all the energy storage of the system; consequently nine eigenvalues are determined for each operating point. For the steady state solution it is enough to use the first six variables since the last three are consequently known.

Table 2 gives the highest eigenvalue and the corresponding T_i and ω_i of the state matrix for different operating points at different frequencies. From this table the system is seen to be stable at the no-load operation for each

Table 2

Frequency cps	T_i p. u.	λ_i (highest value)	T_i p. u.	ω_i p. u.
50	0	$0.994 + j 0.041$	2245	0.040
	0.85	$1.052 + j 0.06$	-20.80	0.054
	-0.85	1.044	-24.60	0
25	0	$0.964 + j 0.155$	88	0.076
	0.85	$1.05 + j 0.10$	-39	0.045
	-0.85	1.069	-31.4	0
5	0	$0.528 + j 0.721$	93.3	0.09
	0.85	0.979	489.7	0
	-0.85	1.219	-52.8	0

frequency, and the lower the frequency, the wider the stability range in the case of motor operation.

I would like to thank Dr. Prof. I. RÁCZ for his available advices throughout this work.

Summary

This paper provides insight into the steady state characteristics of current source inverter/induction motor drive system. Using space state method, an exact solution was obtained by digital computation neglecting the saturation and eddy current effects. This solution is compared to another approximate one [9], based on a simple representation of induction machine and constant dc link current. The stability of the system, is also investigated.

References

1. KOVÁCS, K. P., RÁCZ, I., „Transiente Vorgänge in Wechselstrommaschinen”, I—II. Verlag der Ungarischen Akademie der Wissenschaften, Budapest 1959.
2. RÁCZ, I., „Matrizenberechnung von über Thyristoren gespeisten elektrischen Maschinen” I. Konferenz für Leistungselektronik, No. 2. 1. Vorlesung, Budapest 1970.
3. ZABROVSKI, S. G., LAZAREV, G. B., NATALKIN, A. V., and TOLSTOV, U. G.: “The static characteristics of a frequency control system for an induction motor using current inversion” *Elektrichestvo*, pp. 38—41, Aug. 1971.
4. SPERLING, P. G.: “The static converter fed induction motor operated with impressed square-wave current”, *Siemens-Z.* Vol. 45, pp. 503—514, Aug. 1971.
5. PHILLIPS, K. P.: “Current source converter for ac motor drives” *IEEE. Trans. Ind. Appl.* Vol. IA—8 pp. 679—683, Nov./Dec. 1972.
6. FARRER, W. and MISKIN, J. D.: “Quasi-sine wave fully regenerative inverter”, *Proc. Inst. Elec. Eng.* Vol. 120, pp. 969—976, Sept. 1973.
7. RÁCZ, I.: “Control theory of thyristor connections”. 2nd Conference on Power Electronics, No. 2. 20. Lecture at Budapest, 1973.
8. LIPO, T. A. and CORNELL, E. P.: “State-variable steady state analysis of a controlled current induction motor drive” *IEEE. Trans.* pp. 704—712, Nov./Dec. 1975.
9. LÁZÁR J.: „Berechnung eines Umrichters mit Gleichstromglättung” *Wissenschaftliche Zeitschrift der TH Ilmenau*, Heft 3. pp. 99—129. 22. 1976.

MOHAMED MARWAN EL-SAYED, Helwan University, Cairo, Egypt.